



## CENTRE NATIONAL D'ETUDES SPATIALES

Direction du Centre de Toulouse  
Sous-direction Missions et Exploitation de Données  
Service Observation de la Terre

**THEIA-MU-44-369-CNES**

Edition : 02 Date : 03/12/2020

Révision : 00 Date : 03/12/2020

Code diffusion : E

Réf. :

### GEOV2 AVHRR PRODUCT USER MANUAL

<b>Rédigé par :</b> PACHOLCZYK Philippe VERGER Aleixandre	DCT/ME/OT CREAF	le : 03/12/2020	Validation le 03/12/2020
<b>Validé par :</b>		le :	
<b>Pour application :</b>		le :	

## BORDEREAU D'INDEXATION

CONFIDENTIALITE :

DLP

MOTS CLES :

TITRE DU DOCUMENT :

**GEOV2 AVHRR product User Manual**

AUTEUR(S) :

PACHOLCZYK Philippe

DCT/ME/OT

VERGER Aleixandre

CREAF

RESUME :

DOCUMENTS RATTACHES : Ce document vit seul.

LOCALISATION :

VOLUME : 1

NBRE TOTAL DE PAGES : 19

DOCUMENT COMPOSITE : N

LANGUE : FR

DONT PAGES LIMINAIRES : 0

NBRE DE PAGES SUPPL. : 0

GESTION DE CONF. : Non

RESP. GEST. CONF. :

CAUSE D'EVOLUTION : Distribution des produits jusque 2019

CONTRAT : Néant

SYSTÈME HÔTE :

Microsoft Word 14.0 (14.0.7174)

\\bacchus\GDOC\ModeleGDOC.dot

Version GDOC : v4.3.1.1

Base projet : \\to05res04\GdocBasesPartagees\Projets\CST\PTSC.mdb

## DIFFUSION INTERNE

Nom	Sigle	Bpi	Observations
PACHOLCZYK Philippe	DNO/OT /TA	612	
SPECHT Bernard	DNO/OT /PE	902	
JAUMOUILLE Elodie	DCT/PS/OT	1501	
SELLE Arnaud	DNO/OT /TA	612	

## DIFFUSION EXTERNE

Nom	Sigle	Observations
VERGER Alexandre	CREAF (verger@creaf.uab.cat)	

## MODIFICATION

Ed.	Rév.	Date	Référence, Auteur(s), Causes d'évolution
02	00	03/12/2020	PACHOLCZYK Philippe DCT/ME/OT VERGER Aleixandre CREAM Distribution des produits jusque 2019
01	00	06/08/2019	PACHOLCZYK Philippe DCT/ME/OT VERGER Aleixandre CREAM Création du document

## SOMMAIRE

<b>1.</b>	<b>BACKGROUND .....</b>	<b>1</b>
1.1.	SUMMARY .....	1
1.2.	SCOPE AND OBJECTIVES.....	1
1.3.	DOCUMENTS DE REFERENCE .....	1
<b>2.</b>	<b>ALGORITHM.....</b>	<b>2</b>
1.1.	THE CONSIDERED PRODUCTS .....	2
2.1.1.	FAPAR .....	2
2.1.2.	Cover fraction (FCOVER) .....	2
2.1.3.	Leaf area index (LAI) .....	2
2.2.	THE AVHRR-LTDR DATA .....	3
2.3.	INPUTS .....	5
2.3.1.	Top of canopy normalized reflectances .....	5
2.3.2.	Sun zenith angle .....	5
2.4.	OUTPUT PRODUCT .....	6
2.5.	ALGORITHM OUTLINE .....	6
2.5.1.	Basic underlying assumptions.....	6
2.5.2.	Outline .....	6
2.5.3.	Data preparation (Branch A).....	6
2.5.4.	Processing the time series (Branch B).....	7
<b>3.</b>	<b>PRODUCT DESCRIPTION .....</b>	<b>9</b>
3.1.	FILE FORMAT .....	9
3.2.	PRODUCT CONTENT.....	9
3.3.	PRODUCT CHARACTERISTICS.....	11
3.3.1.	Projection and grid information .....	11
3.3.2.	Temporal information.....	11
3.3.3.	Data policies .....	12
3.3.4.	Contacts .....	12
3.4.	REFERENCES .....	12

## LIST OF ACRONYMS

ATBD	Algorithm theoretical based Document
AVHRR	Advanced Very High Resolution Radiometer
BELMANIP	BEenchmark Land Multisite ANalysis and Intercomparison of Products
BRDF	Bidirectional Reflectance Distribution Function
BS	Bare Soil
CACAO	Consistent Adjustment of Climatology to Actual Observations
CEOS	Committee for Earth Observation Satellite
CGLS	Copernicus Global Land Service
CNES	Centre National d'Études Spatiales (French Space Agency)
CREAF	Centre for Ecological Research and Forestry Applications
CYCLOPES	Carbon cYcle and Change in Land Observational Products from an Ensemble of Satellites
EBF	Evergreen Broadleaf Forest
ECV	Essential Climate Variable
FAPAR	Fraction of Absorbed Photosynthetically Active Radiation
FCOVER	Fraction of vegetation cover
GAC	Global Area Coverage
GAI	Green Area Index
GCOS	Global Climate Observation System
GEOCLIM	Climatology of Version 1 LAI, FAPAR, FCOVER VGT products
GEOV1	GEOLAND2 Version 1 product
GEOV2	GEOLAND2 Version 2 product
GTOS	Global Terrestrial Observation System
INRAE	Institut national de recherche pour l'agriculture, l'alimentation et l'environnement (National Research Institute for Agriculture, Food and Environment, France)
LAC	Local Area Coverage
LAI	Leaf Area Index
LPV	Land Product Validation group of CEOS
LTDR	Long Time Data Record
MODIS	Moderate Imaging Spectrometer
NDVI	Normalized Difference Vegetation Index
NIR	Near Infrared
NNT	Neural Network Technique
QC	Quality control indicator
QF	Quality flag
RMSE	Root Mean Square Error
SPOT	Satellite Pour l'Observation de la Terre
SWIR	Short Wave Infrared
SZA	Sun Zenith Angle
TOC	Top of Canopy
TSGF	Temporal Smoothing Gap Filling
VGT	VEGETATION instrument onboard SPOT satellite
VITO	Vlaamse Instelling voor Technologisch Onderzoek (Flemish Institute for Technological Research), Belgium

## 1. BACKGROUND

### 1.1. SUMMARY

The GEOV2-AVHRR product is a global map of vegetation biophysical variables (FAPAR, LAI and FCOVER) calculated every ten days since 1981 at 0.05° resolution from AVHRR LTDR data.

A first version of the product, called GEOV1-AVHRR, was developed from AVHRR LTDR version 3 data during the FP7 Geoland 2 project (Baret et al. 2011). Some limitations were identified in GEOV1-AHRR product that needed to be corrected.

After this first analysis, it has been decided to adapt the GEOV2 algorithm developed by CREAM and INRAE in the framework of the Copernicus Global Land Service (CGLS) to the characteristics of the AVHRR products to generate GEOV2-AVHRR products. The last version of the code of GEOV2-CGLS algorithm has been delivered by VITO to CNES, which made the necessary software adaptation to the new GEOV2-AVHRR algorithm developed by CREAM with the support of INRAE [DR1].

### 1.2. SCOPE AND OBJECTIVES

The PUM document contains:

- a description of the algorithm (more details can be found in the Algorithm Theoretical Basis Document (ATBD))
- a description of the product: file format, product content, product characteristics.
- a summary of the result of the product validation (the complete results of the validation can be found in the validation report)

### 1.3. DOCUMENTS DE REFERENCE

- DR1            Algorithm Theoretical Basis Document - GEOV2-AVHRR : Leaf Area Index (LAI), Fraction of Absorbed Photosynthetically active Radiation (FAPAR) and Fraction of green Vegetation Cover (FCOVER) from LTDR AVHRR  
**A. Verger (CREAF/INRAE)**  
**THEIA-SP-44-0207-CREAF**
- DR2            GEOV2-AVHRR validation report  
VERGER Alexandre (CREAF/INRAE)**THEIA-RP-44-0281-CREAF**

## 2. ALGORITHM

### 1.1. THE CONSIDERED PRODUCTS

The considered products are called GEOV2-AVHRR and include leaf area index (LAI), the fraction of absorbed photosynthetically active radiation (FAPAR) and the fraction of vegetation cover (FCOVER).

#### 2.1.1. FAPAR

FAPAR corresponds to the fraction of photosynthetically active radiation absorbed by the canopy. The FAPAR value results directly from the radiative transfer model in the canopy, which is computed instantaneously. It depends on canopy structure, vegetation element optical properties and illumination conditions. FAPAR is very useful as input to a number of primary productivity models based on simple efficiency considerations (Prince 1991). Most of the primary productivity models using this efficiency concept are running at the daily time step. Consequently, the product definition should correspond to the daily-integrated FAPAR value that can be approached by computation of the clear sky daily-integrated FAPAR values as well as the FAPAR value computed for diffuse conditions. To improve the consistency with other FAPAR products that are sometimes considering the instantaneous FAPAR value at the time of the satellite overpass under clear sky conditions (e.g. MODIS), a study investigated the differences between alternative FAPAR definitions (Baret et al. 2003). Results show that the instantaneous FAPAR value at 10:00 (or 14:00) solar time is very close to the daily-integrated value under clear sky conditions. To keep a higher consistency with the FAPAR definition used in the CYCLOPES, and MODIS products, the instantaneous FAPAR value at 10:00 solar time under clear sky conditions (equivalent to black-sky conditions as defined also for albedo) was used.

FAPAR is relatively linearly related to reflectance values, and will be little sensitive to scaling issues. Note also that the FAPAR refers only to the green parts of the canopy.

#### 2.1.2. Cover fraction (FCOVER)

It corresponds to one minus the gap fraction for nadir direction. FCOVER is used to separate vegetation and soil in energy balance processes, including temperature and evapotranspiration. It is computed from the leaf area index and other canopy structural variables and does not depend on variables such as the geometry of illumination as compared to FAPAR. For this reason, it is a very good candidate for the replacement of classical vegetation indices for the monitoring of green vegetation. Because of its quasi-linear relationship with reflectances, FCOVER will be only marginally scale dependent (Weiss et al. 2000). Note that similarly to LAI and FAPAR, only the green elements will be considered.

#### 2.1.3. Leaf area index (LAI)

LAI is defined as half the developed area of photosynthetically active elements of the vegetation per unit horizontal ground area. It determines the size of the interface for exchange of energy (including radiation) and mass between the canopy and the atmosphere. This is an intrinsic canopy primary variable that should not depend on observation conditions. LAI is strongly non-linearly related to reflectance. Therefore, its estimation from remote sensing observations will be scale dependent (Garrigues et al. 2006; Weiss et al. 2000). Note that LAI as estimated from remote sensing will include all the green contributors such as the understory when existing under forests canopies. However, except when using directional observations (Chen et al. 2005), LAI is not directly accessible from remote sensing observations due to the possible heterogeneity in leaf distribution within the canopy volume. Therefore, remote sensing observations are rather sensitive to the 'effective' leaf area index, i.e. the value that provides the same diffuse gap fraction while assuming a random distribution of leaves. The



difference between the actual LAI and the effective LAI may be quantified by the clumping index (Chen et al. 2005) that roughly varies between 0.5 (very clumped canopies) and 1.0 (randomly distributed leaves). Note that similarly to the other variables, the retrieved LAI is mainly corresponding to the green element: the correct term to be used would be GAI (Green Area Index) although we propose to still use LAI for the sake of simplicity.

## 2.2. THE AVHRR-LTDR DATA

The Advanced Very High Resolution Radiometer (AVHRR) sensor is an optical instrument that provides multi-spectral imaging by sensing reflected sunlight and thermal emissions.

Several AVHRR sensors have been launched since 1981, which allows getting a long time series. Table 1 gives the temporal coverage since NOAA-7 up to now, for the NOAA satellite used in GEOV2-AVHRR product.

NOAA Satellite Number	Launch date	Ascending Node	Descending Node
7	06/23/1981	1430	0230
9	12/12/1984	1420	0220
11	09/24/1988	1340	0140
14	12/30/1994	1340	0140
16	09/21/2000	1400	0200
18	05/20/2005	1400	0200
19	06/02/2009	2130	0930

**Table 1: Historic of the AVHRR temporal coverage used for GEOV2/AVHRR.**

The AVHRR sensor is nominally a five channel scanning sensor which images in the visible, near infrared and thermal infrared wavelength bands. Band 1 is the visible band, Band 2 is the near infrared band, and Bands 3, 4 and 5 are the thermal bands. Table 2 and Figure 1 indicate the differences of wavelength on each band for each satellite. Note that for the 7 sensors used (7, 9, 11, 14, 16, 18, 19) no SWIR band is available, preventing from improved atmospheric correction.

Band Name	NOAA 7,8,9,10,11,12,14	NOAA 15,16,17,18,19	IFOV (mRad)
1 (Red)	0.58 - 0.68 $\mu\text{m}$	0.58 - 0.68 $\mu\text{m}$	1.39
2 (NIR)	0.725- 1.10 $\mu\text{m}$	0.725-1.0 $\mu\text{m}$	1.41
3A		1.58-1.64 $\mu\text{m}$	1.3

**Table 2: AVHRR spectral characteristics and instantaneous field of view.**

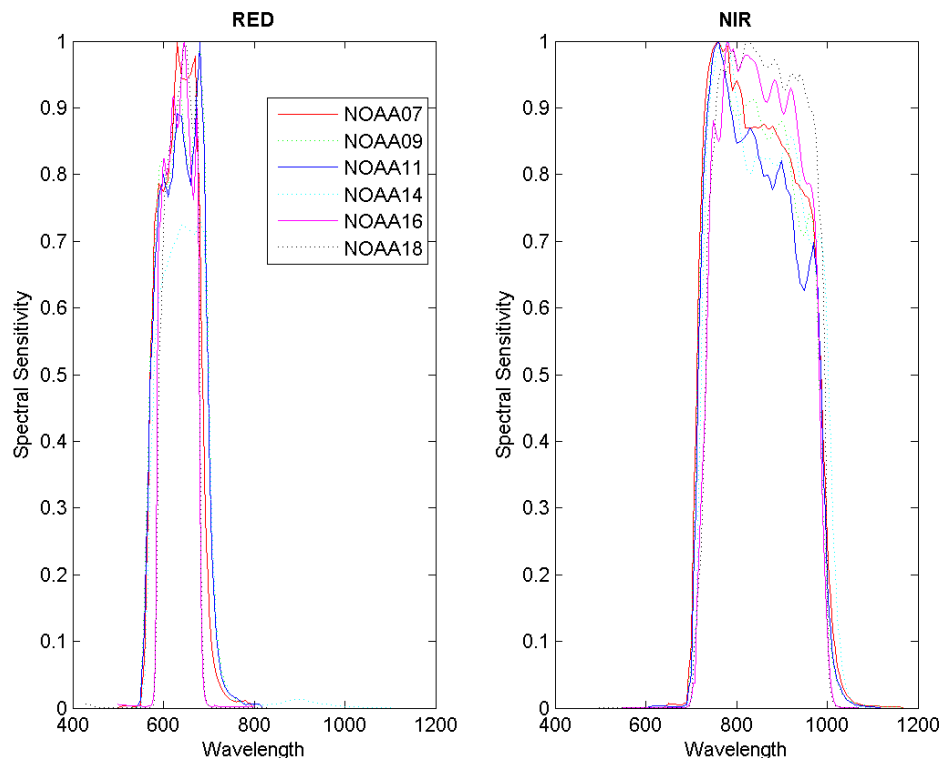


**Figure 1: NOAA07 – NOAA14 spectral responses in the RED (left) and near infrared (right) bands.**

The sensor has a small field of view, scanning across the Earth by the continuous 360 degree rotation of a flat scanning mirror. All the spectral channels are co-registered in order to measure the reflected or emitted energy from the same spot on the earth at the same time. The ground resolution is approximately 1.1 km at the vertical of the satellite from the nominal orbit altitude of about 850 km. The width of off-nadir pixels increases from 1.1 km to about 5 km at the most extreme viewing angle at the edge of the 3000 km imaging swath.

The orientation of the scan lines is perpendicular to the satellite orbit track and the speed of rotation of the scan mirror is selected so that adjacent scan lines are contiguous at the sub-satellite (nadir) position. The satellite speed and scan mirror rotation rate result in an along track pixel height of about 1.1 km. AVHRR data are broadcasted continuously as well as tape-recorded onboard the spacecraft for readout at a NOAA receiving center. The various forms of transmission and area coverage (LAC, GAC) are explained below.

- **LAC** (Local Area Coverage) is nominally 1 km resolution AVHRR imagery recorded with the on board tape recorder for subsequent transmission during the overpass of a station controlled by NOAA. Owing to the large number of data bits, only about 11 minutes of LAC can be accommodated on a single recorder. LAC imagery can only be obtained from NOAA/NESDIS and only in their formats.
- **GAC** (Global Area Coverage) data is lower resolution (4 km) AVHRR imagery. It is derived on board the NOAA satellite by subsampling and averaging the nominal 1 km resolution AVHRR imagery. Out of every 5 normal across track LAC pixels, the 5 bands of the first four are individually averaged and all the bands of the fifth pixel are ignored. In the along track direction, only every third normal line of LAC/HRPT pixels is considered; the two intervening lines are ignored. The GAC spatial resolution is loosely said to be 4 km resolution. It provides anyway a daily global coverage, which is recorded on a satellite tape recorder and then transmitted to a ground station controlled by NOAA. 115 minutes of this lower resolution imagery can be stored on a recorder, enough to cover an entire orbit of data acquisition. GAC imagery can only be obtained from NOAA/NESDIS and only in their formats.

Recently, Vermote and collaborators reanalyzed the GAC data to provide a consistent Long Term Data Record (LTDR) (Vermote and Claverie 2013; Vermote et al. 2010). The LTDR (<http://ltdr.nascom.nasa.gov/ltdr/ltdr.html>) provides better performances than the original GAC data due to the preprocessing improvements identified in the AVHRR Pathfinder II project and the atmospheric corrections used for MODIS.

Top of atmospheric reflectance were first calibrated using the vicarious calibration algorithm (Vermote and Kaufman 1995), cloud screening was applied using the CLAVR-1 algorithm (Stowe et al. 1999) using MODIS thresholds. Atmospheric correction was then performed using water vapor from NCEP data, ozone from TOMS data, Rayleigh scattering from NCEP atmospheric pressure simulations, and aerosols using the red (CH1).

A BRDF normalization was then achieved by applying correction parameters from POLDER in Ross-Li-Maignan model (Maignan et al. 2004). Data are provided for nadir viewing and a 45° solar zenith angle.

LTDR data are provided in hdf format at a daily temporal step and at 0.05° (5.6 km at equator) sampling interval in a latitude/longitude climate modeling grid (CMG). They are dimensioned [7200, 3600].

They correspond to a reasonable hour of ascending crossing time (close to 14:00, see Table 1). Two versions (Version 3 and version 4) for LTDR data are available. LTDR4 geometric performances were improved as compared to LTDR3 and the period has been extended to 2013 (instead of 2000 for LTDR3). Six sensors were used to cover the 1981-2013 period as described in Table 3. In order to have the longest archive with the best accuracy, we used the version 4. However, the LTDR4 dataset presents a gap lasting around almost a year (from 1st January to 2nd November 2000). On the contrary, LTDR3 is available for the entire year 2000. For the year 2000, we used all available LTDR3 and LTDR4 data.

Satellite	Start date (doy)	End date (doy)
NOAA07	1981 176	1985 033
NOAA09	1985 004	1988 312
NOAA11	1988 313	1994 365
NOAA14	1995 001	2000 366
NOAA16	2000 306	2005 365
NOAA18	2005 183	2009 365
NOAA 19	2009 164	2019 056

**Table 3: Sensor used as a function of the year for LTDR data production.**

## 2.3. INPUTS

All these inputs are required for each considered pixel over the time series.

### 2.3.1. Top of canopy normalized reflectances

Top of canopy reflectances normalized for a standard observational configuration (zenith view angle at nadir, sun at 45° as specified in LTDR) are required as inputs. Reflectances should be expressed in terms of reflectance factor, mainly varying between 0 and 0.7 for most land surfaces outside hot-spot or specular directions and snow or ice cover. The red and near infrared AVHRR bands are used. They are provided at 0.05° resolution (≈5.6km<sup>2</sup> at the equator).

### 2.3.2. Sun zenith angle

Since AVHRR LTDR products are directionally normalized for nadir viewing and sun at 45° zenith angle, no information on geometry is required as input to the neural network for LAI and FCOVER. Conversely, since FAPAR is defined as the values at 10:00 local solar time, FAPAR needs the sun zenith angle (actually the cosine of the sun zenith angle is used) at that time as additional input to the neural network. The cosine of the sun zenith angle at

10:00 local solar time needs to be computed as a function of pixel latitude and day in the year. On the other hand, the sun zenith angle at 10:00 local solar time will be used as an input in step 1B (Figure 3) for filtering data at northern high latitudes.

## 2.4. OUTPUT PRODUCT

The outputs are provided by application of the algorithm over each pixel at each dekadal date. They include the LAI, FAPAR and FCOVER values as described previously.

## 2.5. ALGORITHM OUTLINE

### 2.5.1. Basic underlying assumptions

The objective is to develop an algorithm dedicated to the estimation of LAI, FAPAR and FCOVER from the AVHRR series of observations. The algorithm should provide improved products as compared to GEOV1/AVHRR although derived from the same sensors AVHRR/NOAA observations. These LAI, FAPAR and FCOVER products, called here GEOV2-AVHRR, aims to be consistent with GEOV2-CGLS products to ensure continuity. GEOV2/AVHRR should have the same temporal sampling frequency of 10 days. GEOV2-AVHRR capitalizes on the development and validation of already existing CYCLOPES and MODIS products, and the use of neural networks. The basic underlying assumption is that a strong link exists between AVHRR observations and the FUSED products resulting from the fusion of CYCLOPES and MODIS. Products should also be associated with quality assessment flags as well as quantified uncertainties.

### 2.5.2. Outline

The GEOV2-AVHRR algorithm [DR1] starts from the daily LTDR AVHRR daily reflectance products (V4.0). A data preparation process is first completed (Branch A, Figure 2). The output is the instantaneous first guess of the products. Then, temporal techniques are applied to generate the final products at 10-day step (Branch B, Figure 3).

### 2.5.3. Data preparation (Branch A)

The data preparation process is described in Figure 2. It mainly corresponds to a first estimate of instantaneous products (called here Inst. Product1).

1. **Spectral harmonization of AVHRR reflectances (1A)**
2. **Outlier rejection based on inputs (1A).** AVHRR data associated with bad quality flags as well as outside the definition domain used to train the neural networks are removed. This should allow rejecting cloud/snow/water contaminated values.
3. **Deriving daily product estimates using neural networks (2A).** The AVHRR reflectances are transformed into instantaneous products using dedicated neural networks trained over FUSED estimates from CYCLOPES and MODIS products. Inputs are the spectrally corrected AVHRR reflectance values in the red and near infrared (and the cosine of the sun zenith angle at 10h00 only for FAPAR). This will provide consistent time series of daily products. The neural network training process was mainly consisting in the two following main steps:
  - a. The training database was filtered to improve the reliability of the values. This allows defining the definition domain, i.e. the region in the red and near infrared reflectance plan where valid pixels are expected to be located.
  - b. Training the network, i.e. adjusting network architecture and tuning the synaptic coefficients.
  - c. Outlier rejection based on output values (3A): outputs out of the expected physical range are discarded.

4. **Preparation of the climatology (4A).** Knowledge of the climatology as background information is important for the processing of the time series. A climatology was generated at the spatial resolution of AVHRR data based on GEOCLIM, a climatology derived from GEOV1-CGLS (Verger et al. 2015). Further, GEOCLIM is associated with a quality flag (QF) to identify pixels corresponding to evergreen broadleaf forest (EBF) and permanent bare soils (BS). A specific processing is then applied to the EBF and BS time series.

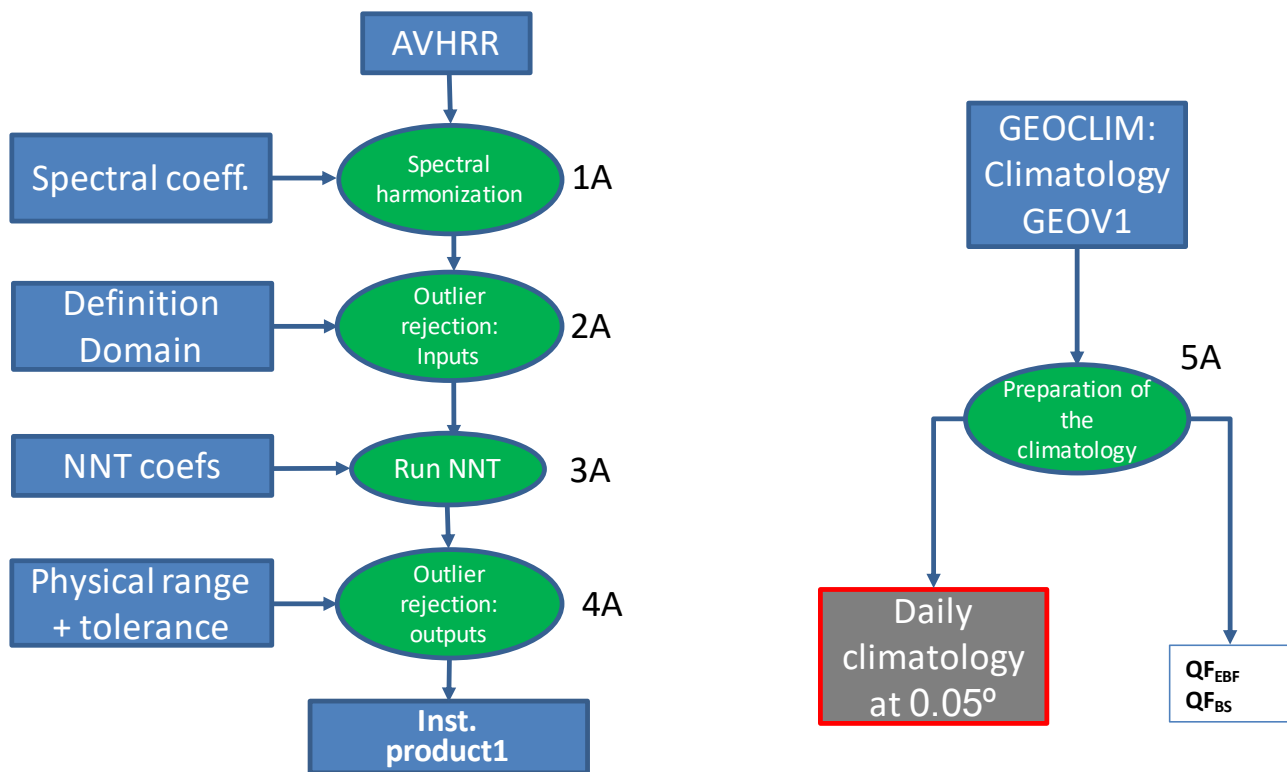


Figure 2: Flow chart describing the data preparation process (Branch A).

## 2.5.4. Processing the time series (Branch B)

The time series processing is described in Figure 3.

1. **Outlier rejection of data for EBF and high northern latitudes (1B).**
2. **Temporal smoothing and gap filling (2B).** The temporal smoothing and gap filling (TSGF) method (Verger et al. 2011) is applied, i.e. a local polynomial fitting within an adaptive window, with (large) gaps filled with the climatology values and a 2 iterations linear interpolation process.
3. **Outlier rejection (3B).** Data which are substantially different from the TSGF series are considered as outliers and thus rejected.
4. **CACAO: Consistent Adjustment of the Climatology to Actual Observations (4B).** The climatology is first decomposed into sub-seasons defined by the minimum and maximum seasonal values observed in the climatology. For each sub-season, the climatology is then adjusted to the available data allowing time shift and magnitude flexibility (Verger et al. 2013). The weighted average values are finally computed over the transition periods (where sub-seasons overlap) to get continuous and smooth products.
5. **Generation of the GEOV2-AVHRR products using TSGF (5B)** for each dekad with the filtered data and CACAO estimates as inputs.

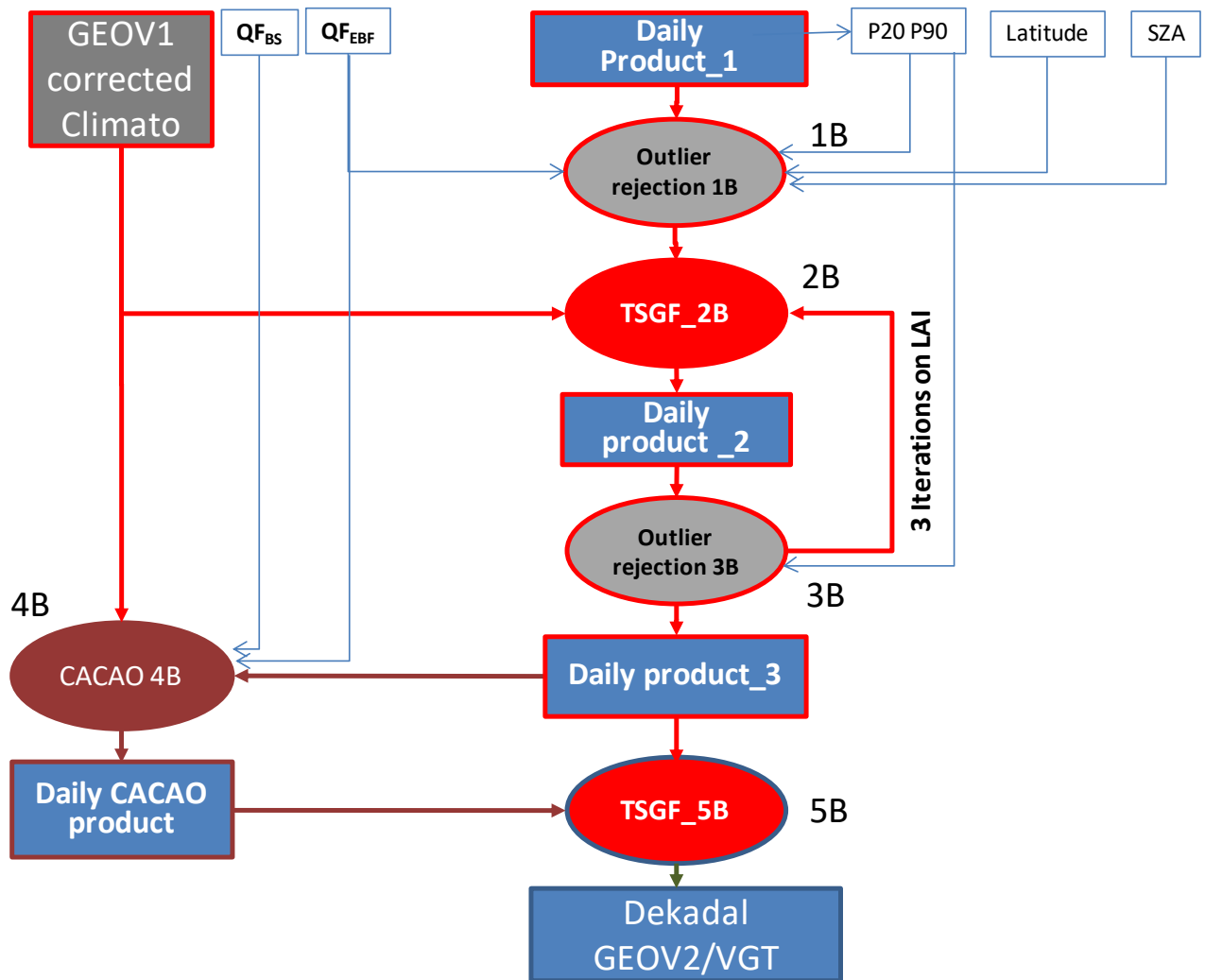


Figure 3: Flow chart describing the processing of the time series (Branch B).

*Daily Product\_1* is coming from step 4A. The resampled GEOCLIM product, i.e. the GEOV1 corrected climatology and the associated quality flags  $QF_{EBF}/QF_{BS}$ , come from step 4A. The sun zenith angle (SZA) at 10:00 local solar time was computed in step 2A.

### 3. PRODUCT DESCRIPTION

The GEOV2-AVHRR product files follow the name convention:

THEIA\_GEOV2\_Rnn\_AVHRR\_pppppp\_yyyymmdd.h5.gz

With :

- nn = version number with two digits
- pppppp = type of parameter: « LAI », « FAPAR » ou « FCOVER »
- yyyymmdd = product date,

Products are generated on day 5, 15 and 25 of each month.

#### 3.1. FILE FORMAT

The LAI, FAPAR, FCOVER GEOV2-AVHRR Theia products are distributed in zip archives. The archive contains multi-band HDF-5 file containing the following layers, with pppppp = type of parameter: « LAI », « FAPAR » ou « FCOVER » :

- pppppp : value of the biophysical variable
- pppppp-RMSE : root mean square error of the final dekadal product value for each variable as compared to the available daily estimates in the composition period
- pppppp-QFLAG : quality flag
- pppppp-NOBS : number of valid LTDR observations in the compositing window
- pppppp-SEMI-PER-LEFT and pppppp-SEMI-PER-RIGHT: length in days of left and right semi-period (before and after the dekadal date) of the compositing window.

Each file corresponds to a global map.

TIPS: You can download and install HDF5 library from <http://www.hdfgroup.org>.

The library comes with useful tools that could be used to discover the organization and contents of the hdf5 files.

You can also download a java viewer called HDFView from the same URL. This tool is more user friendly oriented than the line commands.

#### 3.2. PRODUCT CONTENT

The physical range of LAI, FAPAR, and FCOVER is given in Table 4 and the physical range of the quality indicators in Table 5.

The physical values are retrieved by:

$$DN = \text{PhyVal} * \text{ScalingFactor} + \text{Offset}$$

where the scaling factor and the offset are given in Table 4.

The range of variation and resolution proposed are presented in Table 4. The same conventions as for GEOV2-CGLS are used here. Invalid values are set to 255.

Variable	Physical Minimum	Physical Maximum	Max DN value	Scaling factor	Offset
LAI	0.0	7.0	210	30	0
FAPAR	0.0	0.94	235	250	0
FCOVER	0.0	1.0	250	250	0

**Table 4: Minimum, maximum values and associated resolution for LAI, FAPAR and FCOVER products.**

In addition to the product values, other quantitative quality indicators and quality flags are also generated (Table 5).

Variable	Physical Minimum	Physical Maximum	Max DN value	Scaling factor	Offset
NOBS	0.0	120	120	1	0
SEMI-PER-LEFT	30	60	60	1	0
SEMI-PER-RIGHT	30	60	60	1	0
LAI-RMSE	0.0	7.0	210	30	0
FAPAR-RMSE	0.0	0.94	235	250	0
FCOVER-RMSE	0.0	1.0	250	250	0

**Table 5: Minimum, maximum values and associated resolution for LAI, FAPAR and FCOVER quantitative quality indicators.**



The quality flag (QFLAG) description is given in the following table.

Bit #	Description if set to 0	Description if set to 1
0	Unused	
1 : processed	The pixel is processed (land)	The pixel is unprocessed (water)
2 : climatology value	A climatology value exist for the pixel	No climatology value for the pixel
3 : filling	No filling procedure	The number of valid observations at least on one side of the $\pm 60$ -day period is lower than 6 and a gap filling procedure (Bit 13-14) is applied
4	Reserved	
5	Reserved	
6 : input status	At least one valid data within $\pm 60$ days	No valid data within $\pm 60$ days
7 : LAI status	OK	Out of range or invalid
8 : FAPAR status	OK	Out of range or invalid
9 : FCOVER status	OK	Out of range or invalid
10 : SZA status	$SZA \leq 70$ or latitude $\leq 55$	$SZA > 70$ and latitude $> 55$
11 : EBF status	Pixel is not recognized as Evergreen Broadleaf Forest	Pixel is recognized as Evergreen Broadleaf Forest
12 : BS status	Pixel is not recognized as Bare Soil	Pixel is recognized as Bare Soil
13 : climatology filled	Not filled	Filled with climatology
14 : gap filled	Not filled	Filled with interpolation
15	Unused	

**Table 6: Description of the quality flag for LAI, FAPAR and FCOVER.**

The QFLAG bits are calculated only if bit 1 is set to 0.

### 3.3. PRODUCT CHARACTERISTICS

#### 3.3.1. Projection and grid information

The product is displayed in a regular latitude/longitude grid (plate carrée) with the ellipsoid WGS 1984 (Terrestrial radius=6378km). The resolution of the grid is  $0.05^\circ$ .

The reference is the centre of the pixel. It means that the longitude of the upper left corner of the pixel is (pixel\_longitude – angular\_resolution/2.)

Each file covers the entire globe, which corresponds to an array of 7200 lines by 3600 columns.

#### 3.3.2. Temporal information

The GEOV2-AVHRR products are updated every 10 days using a moving and flexible compositing window within  $\pm$

60-days. The temporal information “YYYYMMDD” in the filename is the “actual” date corresponding to the product value. The “actual” date is the date to take in consideration for any analysis.

### 3.3.3. Data policies

Any use of the original GEOV2-AVHRR Theia products implies the obligation to include in any publication or communication using these products the following citation:

“GEOV2-AVHRR was produced and distributed by CNES based on the algorithm developed by CREAM and INRAE, in the framework of the Theia Land Data Centre.”

The user accepts to inform Theia about the outcome of the use of the above-mentioned products and to send a copy of any publications that use these products to the following address : [theia-land@cnes.fr](mailto:theia-land@cnes.fr)

### 3.3.4. Contacts

Scientific contact : CREAM : Centre de Recerca Ecològica i Aplicacions Forestals, Barcelona, Spain.

Email address: [verger@creaf.uab.cat](mailto:verger@creaf.uab.cat)

Production: CNES : Centre National d'Etudes Spatiales, Toulouse, France

Email address: [theia-land@cnes.fr](mailto:theia-land@cnes.fr)

## 3.4. REFERENCES

Baret, F., Leroy, M., Roujean, J.L., Knorr, W., Lambin, E., & Linderman, M. (2003). CYCLOPES User Requirement Document. In. Avignon: INRA-CSE

Baret, F., Verger, A., & Weiss, M. (2014). Algorithm Theoretical Basis Document Leaf Area Index (LAI), Fraction of Absorbed Photosynthetically Active Radiation (FAPAR) and Fraction of green Vegetation Cover (FCover). Version 2.0 (GEOV2). In (p. 71). Avignon: INRA-EMMAH

Baret, F., Weiss, M., & Kandasamy, S. (2010). Climatology of LAI, FAPAR and FCOVER products (V1). In (p. 30). Avignon (France): INRA-EMMAH

Baret, F., Weiss, M., Lacaze, R., Camacho, F., Makhmara, H., Pacholczyk, P., & Smets, B. (2013). GEOV1: LAI, FAPAR Essential Climate Variables and FCOVER global time series capitalizing over existing products. Part1: Principles of development and production. *Remote Sensing of Environment*, 137, 299-309

Baret, F., Weiss, M., Verger, A., & Kandasamy, S. (2011). BioPar Methods Compendium - LAI, FAPAR and FCOVER from LTDR AVHRR series. In, Report for EC contract FP-7-218795. Available at <http://www.geoland2.eu/portal/documents/CA80C881.html> (p. 46). Avignon: INRA-EMMAH

Chen, J.M., Menges, C.H., & Leblanc, S.G. (2005). Global mapping of foliage clumping index using multi-angular satellite data. *Remote Sensing of Environment*, 97, 447-457

Garrigues, S., Allard, D., Baret, F., & Weiss, M. (2006). Influence landscape spatial heterogeneity on the non-linear estimation of leaf area index from moderate spatial resolution remote sensing data. *Remote Sensing of Environment*, 105, 286-298

Maignan, F., Bréon, F.M., & Lacaze, R. (2004). Bidirectional reflectance of Earth targets: evaluation of analytical models using large set of spaceborne measurements with emphasis on the hot-spot. *Remote Sensing of Environment*, 90, 210-220

Prince, S.D. (1991). A model of regional primary production for use with coarse resolution satellite data. *International Journal of Remote Sensing*

Roujean, J.L., Leroy, M., & Deschamps, P.Y. (1992). A bidirectional reflectance model of the Earth's surface for the correction of remote sensing data. *Journal of Geophysical Research*, 97, 20455-20468

Stowe, L.L., Davis, P.A., & McClain, E.P. (1999). Scientific basis and initial evaluation of the CLAVR-1 global clear/cloud classification algorithm for the advanced very high resolution radiometer. *Journal of Atmospheric and Oceanic Technology*, 16, 656-681

Verger, A., Baret, F., & Weiss, M. (2011). A multisensor fusion approach to improve LAI time series. *Remote Sensing of Environment*, 115, 2460-2470

Verger, A., Baret, F., & Weiss, M. (2014). Near real time vegetation monitoring at global scale. *IEEE Journal of Selected Topics in Applied Earth Observations and Remote Sensing*, 7, 3473-3481

Verger, A., Baret, F., Weiss, M., Kandasamy, S., & Vermote, E. (2013). The CACAO method for smoothing, gap filling and characterizing seasonal anomalies in satellite time series. *IEEE transactions on Geoscience and Remote Sensing*, 51, 1963-1972

Verger, A., Baret, F., Weiss, M., Filella, I., & Peñuelas, J. (2015). GEOCLIM: A global climatology of LAI, FAPAR, and FCOVER from VEGETATION observations for 1999–2010. *Remote Sensing of Environment*, 166, 126-137

Vermote, E., & Claverie, M. (2013). Climate Algorithm Theoretical Basis Document. AVHRR Land Bundle - Surface Reflectance and Normalized Difference Vegetation Index. In (p. 38): NOAA

Vermote, E., Justice, C., Csiszar, I., Eidenshink, J., Mynemi, R., Baret, F., Masuoka, E., & Wolfe, R. (2010). A terrestrial surface climate data record for global change studies. In J. Sobrino (Ed.), *Third International Symposium on Recent Advances in Quantitative Remote Sensing*. Torrent (Spain)

Vermote, E., Justice, C., Csiszar, I., Eidenshink, J., Myneni, R., Baret, F., Masuoka, E., & Wolfe, R. (2009). A Terrestrial Surface Climate Data Record for Global Change Studies. In, *Fall Meeting, San-Francisco (USA): Eos Transactions, Suppl.*, v. 90, no. 52: Washington, D.C., American Geophysical Union, abstract number IN42A-08. (Also available online at <http://www.agu.org/meetings/fm09/waisfm09adv.html>.)

Vermote, E., & Kaufman, J.K. (1995). Absolute calibration of AVHRR visible and near-infrared channels using ocean and cloud views. *International Journal of Remote Sensing*, 16, 2317-2340

Weiss, M., Baret, F., Myneni, R., Pragnère, A., & Knyazikhin, Y. (2000). Investigation of a model inversion technique for the estimation of crop characteristics from spectral and directional reflectance data. *Agronomie*, 20, 3-22

Zhu, Z., Bi, J., Pan, Y., Ganguly, S., Anav, A., Xu, L., Samanta, A., Piao, S., Nemani, R., & Myneni, R. (2013). Global Data Sets of Vegetation Leaf Area Index (LAI)<sub>3g</sub> and Fraction of Photosynthetically Active Radiation (FPAR)<sub>3g</sub> Derived from Global Inventory Modeling and Mapping Studies (GIMMS) Normalized Difference Vegetation Index (NDVI)<sub>3g</sub> for the Period 1981 to 2011. *Remote Sensing*, 5, 927-948